Multilayer gold nanoparticle-assisted thermal desorption ambient mass spectrometry for the analysis of small organics

Jia-Yi Lin, Tsung-Yi Chen, Jen-Yi Chen and Yu-Chie Chen*

Received 17th March 2010, Accepted 13th July 2010
DOI: 10.1039/c0an00157k

In this study, thermal desorption-based ambient mass spectrometry (TDAMS) for the analysis of small organics was explored. A layer-by-layer (LBL) self-assembled multilayer of a gold nanoparticle (AuNP)-based glass chip (Glass@AuNPs) with the absorption capacity in the near-infrared (NIR) region was used as the energy absorber and as the sample holder for sample deposition at ambient condition. An NIR laser diode (808 nm) was successfully employed as the thermal desorption source to liberate only small molecules from Glass@AuNPs chips. Followed by post-ionization, the resultant ions were monitored by an ion trap mass spectrometer. Post-ionization was assisted by a spray consisting of 50% deionized water–acetonitrile containing 0.1% acetic acid generated from a short tapered capillary by employing a high voltage (4 kV). Analytes with different polarities including small acids, amino acids, insecticides, and biodiesel samples such as ethyl esters can be directly analyzed using this approach. We demonstrated that this ambient mass spectrometric method was suitable for selectively analyzing small target organics directly from complex samples without any sample pretreatment.

Introduction

Spherical gold nanoparticle (AuNP)-based localized surface plasmon resonance (LSPR) generally has a broad band across the ultraviolet (UV) region accompanying a notable absorption band appearing in the visible region.[1,2] On the basis of the absorption capacity in the UV region, AuNPs have lately been explored as the assisting material in surface-assisted laser desorption/ionization mass spectrometry (SALDI MS),[3–8] which generally uses inorganic materials including graphite,[9,10] titania,[11–13] and iron oxide NPs[14] capable of absorbing the UV laser energy as the assisting materials for laser desorption/ionization of analytes. It has been demonstrated that AuNPs can be used to assist the analysis of biomolecules effectively including peptides,[3] proteins,[3,4] and small molecules such as aminothiols,[5] neutral small carbohydrates,[6] adenosine triphosphate (ATP),[7] and glutathione[8] in SALDI MS.

When fabricating layer-by-layer (LBL) self-assembled AuNPs on glass slides (Glass@AuNPs), the absorption intensity of the broad band in the UV region is enhanced, and a new absorption band occurs in the near infrared (NIR) arising from the dipole–dipole interactions between AuNPs.[15–17] Arakawa and co-workers[8] employed the LBL self-assembled AuNP-multilayer films as effective SALDI-assisting materials for the analysis of peptides and proteins based on the enhanced absorption intensity in the UV region. The absorption capability appearing in the NIR region of the LBL self-assembled AuNP multilayer films can be used in the design for thermal desorption mass spectrometry by alternatively using an NIR laser as the irradiation source. On the basis of this premise, we explored a new type of ambient mass spectrometry in this study.

Ambient mass spectrometry (MS)[18–25] has lately attracted a great deal of attention because it allows for direct analysis at atmospheric pressure without any pretreatment or with only minimum sample preparation, offering the advantages of speed and ease-of-use. For example, the development of desorption electrospray ionization (DESI)[18] by Cooks's research group has made a great impact in the progress of ambient MS. A fine spray of charged droplets is used as the desorption/ionization source for analytes without any sample preparation under ambient conditions. Direct analysis in real time (DART),[19] electrospray-assisted laser desorption/ionization (ELDI),[20] an atmospheric solid analysis probe (ASAP),[21] laser diode thermal desorption (LDTD),[22] extractive electrospray ionization (EESI),[23] low temperature plasma (LTP) ionization,[24] easy ambient sonic-spray ionization (EASI) MS,[25] atmospheric-pressure thermal desorption ionization (APTDI),[26] and atmospheric pressure femtosecond laser imaging MS[27] have also demonstrated the usefulness of ambient MS for various types of analytes. In this study, we proposed the use of Glass@AuNPs to the design of thermal desorption ambient MS (TDAMS). On the basis of the absorption capability of the Glass@AuNPs chip in the NIR region, the chip was used as the sample holder for sample deposition and as the energy absorber. An NIR laser diode was used as the energy source for volatilizing samples from the chip. Generally, when thermal desorption (TD) is employed to volatilize intact thermo-labile analytes, it can only selectively desorb analytes with molecular masses up to several hundred Daltons. Thus, employing TD as the desorption source for mass spectrometric analysis may be limited to the analysis of low mass analytes with moderate polarities. Taking this feature another way, it may be seen as an advantage when considering it in terms of selectivity. Since

Department of Applied Chemistry, National Chiao Tung University, Hsinchu, 300, Taiwan. E-mail: yuchie@mail.nctu.edu.tw; Fax: 886-3-5723764; Tel: 886-3-5131527

TD selectively volatilizes only low molecular weight organics, it can be employed as a method to selectively liberate small molecules from complex samples. The contribution from non-target molecules with large masses can be eliminated owing to the incapability of TD in volatilizing large organics. Therefore, the interference arising from the large molecules can be reduced. The steps of sample extraction and pretreatment may be eliminated. Therefore, the analysis time can be shortened. In this study, we initially demonstrated the feasibility of using this new ambient MS method for the analysis of small organics with low to high polarity. Furthermore, direct analysis of trace analytes from complex samples and reaction products without sample pretreatment was also conducted.

Experimental

Reagents and materials

All amino acids, citric acid, ferulic acid, malic acid, and syringic acid were purchased from Sigma (St. Louis, MO, USA). *N*-[3-(trimethoxysilyl)propyl]ethylenediamine (EDAS) was purchased from Aldrich (Milwaukee, WI, USA). Acetonitrile, methanol, acetic acid, hydrochloric acid (35%), hydrofluoric acid (48%), and trifluoroacetic acid were obtained from Merck (Darmstadt, Germany). Sodium hydroxide and 2-propanol were purchased from J. T. Baker (Phillipsburg, NJ, USA). Sulfuric acid (95%), trisodium citrate, and hydrogen peroxide (35%) were purchased from Riedel-de Haën (Seelze, Germany). Acephate, nitric acid (65%), and methamidophos were purchased from Fluka (St. Gallen, Switzerland). Hydrogen tetrachloroaurate(III) tetrahydrate ($HAuCl_4$) was obtained from Showa (Tokyo, Japan). Human serum was donated by a healthy individual from Mackay Memorial Hospital (Hsinchu, Taiwan). Ethanol was obtained from Showa (Tokyo, Japan). The fused silica capillary (inner diameter: 50 μm, outer diameter: 366 μm) was purchased from Polymicro Technologies Inc. (Phoenix, AZ, USA). Glass cover slides (18 mm × 18 mm × 0.15 mm) were purchased from Matsunami (Osaka, Japan). Soybean oil was purchased from a local grocery store.

Fabrication of Glass@AuNPs chips

AuNPs were prepared using the Frens method.[28] All the glassware and stirring bars were rinsed with a solution consisting of HNO_3 (65%)/HCl (35%) (1/3, v/v) and then by deionized water. An aqueous tetrachloroaurate solution (0.1 mg mL^{-1}, 50 mL) was heated to boiling point, and trisodium citrate (0.1%, 0.3 mL) was added to the solution while stirring. Initially, the solution turned to a blue color when AuNPs were generated, this indicated aggregations of the newly generated AuNPs.[28] When the color of the AuNP suspension became red, it indicated the formation of monodisperse spherical particles.[28] The solution was heated continuously while stirring for an additional 5 min after the color of the solution had changed to red. After cooling to room temperature, the suspension of AuNPs was centrifuged at 2,500 rpm for 10 min. The supernatant was removed by pipette. The remaining NPs were re-suspended in a small amount of deionized water. The suspension (0.1 mL) was diluted to obtain optical density (O.D.) ~6 at a wavelength of 540 nm.

Glass slides were pretreated by soaking in a piranha solution [3 : 1 (v/v) H_2SO_4 (95%)/H_2O_2(35%)] for 30 min to remove impurities and then washed with water and methanol under sonication. The piranha solution is highly reactive, and thus it should be handled with care. The glass slides were stored in methanol before use. The slides were then dried by a hair dryer before surface modification. The surface of the glass slide was modified with a thin film of EDAS by depositing with 0.5 mL of EDAS (0.25% (v/v)) prepared in deionized water for 10 min. The slide was rinsed with deionized water to remove unbound EDAS, dried with a hair dryer, and heated in an oven at 120 °C for 1 h. The surface of the slide was coated with the AuNP suspension (0.2 mL) prepared above *via* electrostatic interactions after the slide was cooled to room temperature. After standing at ambient temperature for 12 h, the slide was rinsed with deionized water to remove unbound AuNPs and was dried using a hairdryer. EDAS and AuNPs were then repeatedly coated on the surface of the slide twice to generate a three-layered Glass@AuNPs slide. The steps for fabrication of the Glass@AuNPs were illustrated in Scheme 1.

Fabrication of an ESI capillary emitter

A pulled bare-fused silica capillary (length: ~4 cm) was fabricated and used as the ESI emitter. We initially conditioned a capillary (length: ~80 cm) by using a pump (pressure: 18 mmHg) to rinse it successively with 0.1 N NaOH (30 min) and water (30 min). Approximately 5 cm of pulled bare-fused silica capillary was fabricated by applying a small weight (50 g) on the lower end of the vertical capillary that had been conditioned above. The lower part of the capillary was heated by a Rekrow butane flame gun (Micro Torch-RK2050, Taipei, Taiwan) and was quickly drawn to form a narrow capillary tip. After cooling to room temperature, the capillary tip was immersed in an HF solution (24%) for 10 min. The tip (i.d.: ~10 μm; o.d.: ~20 μm) was washed with methanol and deionized water, and the short tapered capillary was then flushed with deionized water using a pump for 10 min. The short capillary was then cut to 4 cm and quickly placed in an Eppendorf tube, which had been drilled to a small hole on the wall, containing the ESI solution (see Scheme 2).

Configuration of the TDAMS system

Scheme 2 presents the configuration of the TDAMS system incorporating the pulled bare capillary as the ESI emitter for post-ionization. This setup consists of a power supply, a short tapered-capillary, a platinum electrode, an Eppendorf tube containing the ESI solution, a Glass@AuNPs chip, an NIR laser diode (808 nm, 1 W) (UrMap, Hsinchu, Taiwan) equipped with an optical fiber (200 μm), and an ion trap mass spectrometer. The short-tapered capillary, which was used as the spray emitter, was placed *ca.* 2 mm above the Glass@AuNPs chip and distanced *ca.* 4 mm from the inlet orifice of the mass spectrometer. No electrical contact was applied on the outlet of the capillary tip. The capillary inlet was placed in an Eppendorf tube containing the ESI solution and a platinum electrode connected to a high-voltage power supply (4 kV) when operating at positive ion mode. The ESI solution was comprised of water–acetonitrile (1/1, v/v) containing 0.1% acetic acid. The NIR laser was placed *ca.* 5 mm below the Glass@AuNPs chip. The temperature on the

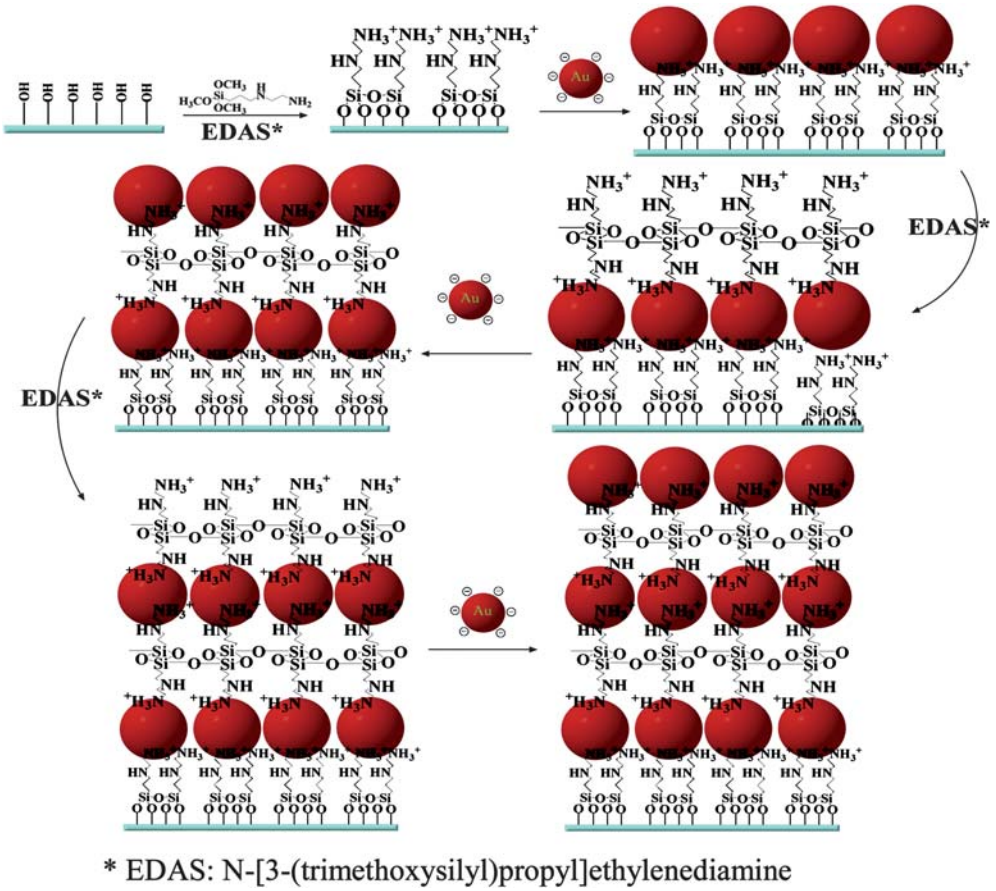

Scheme 1 Cartoon representation of the steps for fabrication of Glass@AuNPs slide.

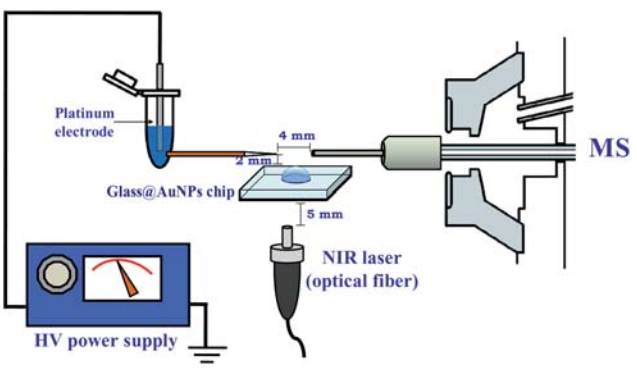

Scheme 2 Cartoon representation of the setup of the TDAMS system. An NIR laser was used to irradiate the rear side of the Glass@AuNPs chip to liberate samples followed by post-ionization with electrospray. The spray consisting of deionized water–acetonitrile (1/1, v/v) containing 0.1% acetic acid was generated from a short-tapered capillary tip, while the capillary inlet was connected to 4 kV. When operating at positive ion mode, −500 V was set at MS.

chip was measured by Raytek-MT4 (Santa Cruz, CA, USA), while the output power of the NIR laser was measured by a Coherent PM-10 Laser Power Meter (Santa Clara, CA, USA).

Preparation of biodiesel samples

The transesterification reaction of soybean oil was performed based on a method reported previously.[29] Ethanol (800 μL), soybean oil (200 μL), and sodium hydroxide (1 μL, 2 N) were mixed in a sample vial under ultrasonication (40 kHz) for 30 min at room temperature. The resultant solution was diluted 1000-fold by 2-propanol before MS analysis.

Instrumentation

All the absorption spectra were obtained from a Varian Cary 50 ultraviolet (UV)/visible (Vis) absorption spectrophotometer (Melbourne, Australia). Scanning electronic microscopy (SEM) images were obtained using a JEOL JSF-6500F SEM (Tokyo, Japan). All the mass spectra were obtained using an Esquire 2000 (Bruker Daltonics, Leipzig, Germany). NanoESI on-line mode was selected. Optical images were obtained using an Eclipse 80i (Nikon, Yokohama, Japan).

Results and discussion

We first fabricated the Glass@AuNPs chip with AuNPs by initially modifying the surface of a thin glass slide with EDAS, which contains amino-terminal functional groups. AuNPs (50.5 ± 4.3 nm) with negatively charged functionalities were then attached onto the surface of the chip *via* electrostatic interactions. The second layer of EDAS was immobilized onto the surface of AuNPs, followed by interaction with the other layer of AuNPs. A layer of EDAS attached to AuNPs was then immobilized onto the chip. Fig. 1a shows the corresponding absorption spectra from layer to layer. There is a maximum absorption

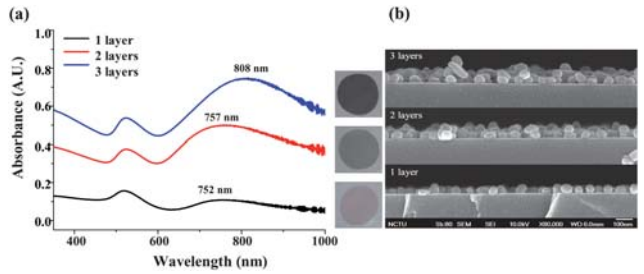

Fig. 1 Absorption spectra and corresponding photographs of layer-by-layer self-assembled Glass@AuNPs chips. (b) SEM images of the cross section of Glass@AuNPs from one layer-coating to three layer-coating (bottom to top).

band appearing at the wavelength of ~522 nm when modifying the first layer of AuNPs on the glass chip. The corresponding photograph adjacent to this absorption spectrum displays that the glass slide coated with the first layer of AuNPs in red. When further modifying the surface of the chip with a second layer of AuNPs, a new absorption band is revealed at ~757 nm arising from the dipole–dipole interactions between AuNPs. Apparently, the modified chip becomes blue. As the third layer of AuNPs is immobilized on the chip, the maximum absorption band in the NIR region has a red shift to ~808 nm with increased intensity. The resultant chip looks dark in the photograph. Fig. 1b presents the corresponding SEM images of the cross sections of the chip immobilized with layer-by-layer of AuNPs (from the bottom to top). The chip with the maximum absorption band in the NIR region was then successfully generated as we desired. The coverage of AuNPs on the surface of the chip from the first layer, the second layer, and the third layer coating was estimated at 33.8%, 52.9%, and 74.4%, respectively. The estimation was based on the ratio % of the surface area covered by the AuNPs on that of the glass slide.

The as-prepared chip was then employed as TD substrate by holding samples on one side and heating by an NIR diode laser (808 nm) on the other side, which had been immobilized with the LBL self-assembled AuNPs. Scheme 2 displays the configuration of the TDAMS system. We employed an electrospray consisting of water–acetonitrile containing 0.1% acetic acid generated from a short tapered-capillary[30–32] by applying a high electric field to the capillary inlet for post-ionization of the gas species desorbed from the chip. We initially used small polar acids as samples to examine the feasibility of using this approach in MS analysis. Fig. 2a–c present negative ion mode mass spectra of citric acid, ferulic acid, and syringic acid obtained from TDAMS. Deprotonated pseudomolecular ions of these acids dominate the mass spectra. The ions at *m/z* 172.9 and 111.1 were derived from the fragmentation of citric acid appearing in the mass spectrum, as shown in Fig. 2a. The deprotonated pseudomolecular ions ($[M - H]^-$) and dimer ions ($[2M - H]^-$) derived from ferulic acid and syringic acid are presented in the mass spectra of Fig. 2b and 2c, respectively. The results indicate that our design is suitable for the analysis of these thermal labile and polar organic acids. In addition, intact molecular ions are the only peaks observed in most of the TDAMS spectra. However, for analytes with fragile functional groups, their fragments may be observed in the same mass spectra (Fig. 2a).

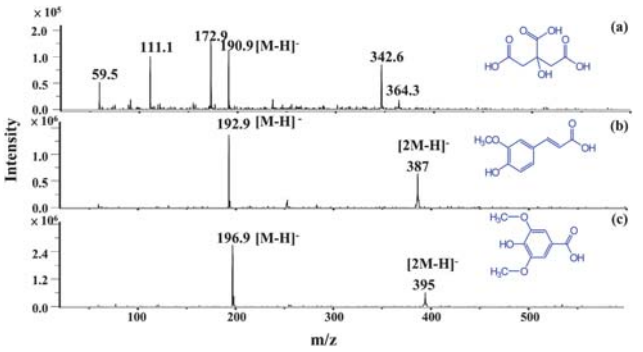

Fig. 2 TDAMS spectra of small acids (1 mM, 2 μL): (a) citric acid (mw = 192.1), (b) ferulic acid (mw = 194.2), and (c) syringic acid (mw = 198.2).

To demonstrate the requirement of the use of post-ionization spray in this approach, we used malic acid ($[M - H]^- = 133$) as the sample by switching the ESI spray on and off during mass spectrometric analysis. Fig. 3a and 3b present the total ion current chromatogram (TIC) and extracted ion chromatogram (EIC) at *m/z* 133, respectively. Fig. 3c and 3d show the corresponding mass spectra obtained during the spray-off and spray-on, respectively. Apparently, when the spray is turned off, the ion signals of malic acid at *m/z* 133 totally disappear. Upon switching the spray on, the ion signals appear in the mass spectrum. The results demonstrate that post-ionization is required to ionize the gas species generated by thermal desorption. Additionally, the flow generated by electrospray also can readily direct the gas ion species into the mass spectrometer. We also monitored the signal changes by switching the NIR laser on and off during mass spectrometric analysis. The NIR laser was positioned *ca.* 5 mm below the glass chip, and its power output was measured *ca.* 153 mW at this distance with the laser beam area of 0.3 cm^2. Malic

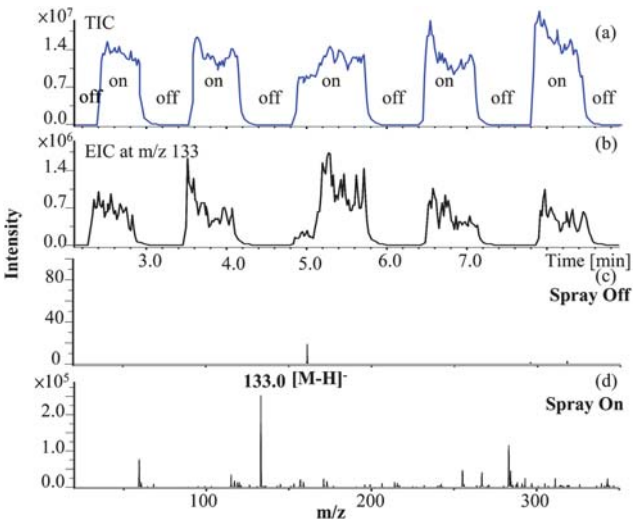

Fig. 3 Plots of (a) total ion monitoring (TIC) and (b) extracted ion chromatogram (EIC) at *m/z* 133 as a function of time by switching the spray on/off. Aqueous malic acid (1 mM, $[M - H]^- = 133$) was used as the sample. Mass spectra were obtained by switching the spray (c) off and (d) on.

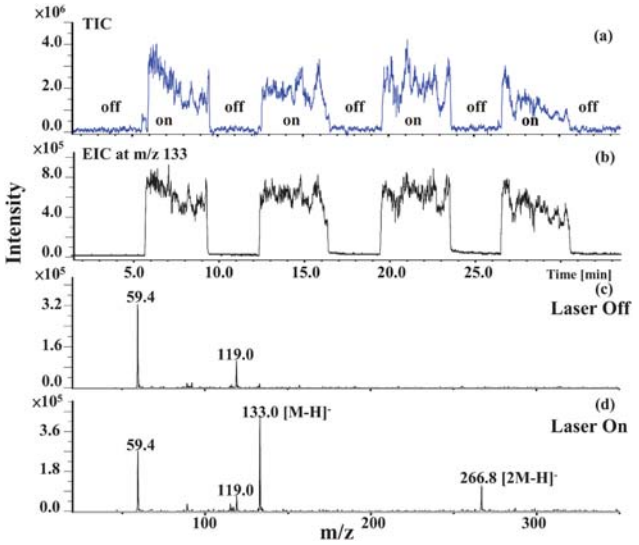

Fig. 4 Plots of (a) total ion monitoring (TIC) and (b) extracted ion chromatogram (EIC) at *m/z* 133 as a function of time by switching the NIR laser on/off. Aqueous malic acid (1 mM, $[M - H]^- = 133$) was used as the sample. Mass spectra were obtained during switching the NIR laser (c) off and (d) on.

acid was still used as the sample for examination. Fig. 4a and 4b present the TIC and EIC at *m/z* 133, respectively. The ion signals of malic acid at *m/z* 133 only appeared upon switching the NIR laser on. Fig. 4c and 4d display the mass spectra of malic acid as the NIR laser is turned off and on, respectively. The mass spectral results also confirm that the analyte ion at *m/z* 133 only appears as the NIR laser is turned on. The detection limit is as low as 200 fmol (10^{-7} M, 2 μL), which is slightly lower than that obtained from the existing techniques such as atmospheric pressure imaging mass spectrometry.[28] In that study, the detection limit for a small organic acid was ~500 fmol.[28] In addition, these results indicate that both NIR laser and post-ionization spray are required components for this current approach.

To study systematically the feasibility of this ambient MS for different types of analytes, 20 amino acids with different polarities were examined. The results demonstrate that almost all the amino acids that belong to the category with hydrophobic functional groups, including alanine, proline, valine, isoleucine, leucine, methionine, and phenylalanine, can be readily analyzed using TDAMS. Regarding hydrophilic types of amino acids, only glycine, threonine, cysteine, and cystine can be observed in the TDAMS spectra. Among negatively charged and positively charged amino acids, only glutamic acid can be obtained using this approach. The results show that TDAMS does not favor for the analysis of the analytes with high polarities. Protonated and deprotonated molecular ions of these amino acids can be readily obtained in the positive ion mode and negative ion mode of mass spectra, respectively. The detection limit for these amino acids such as leucine is as low as 200 fmol (10^{-7} M, 2 μL).

As we proposed that one of the main advantages of this ambient MS is its capability to detect small and thermally labile analytes from complex samples selectively, sera spiked with amino acids, including leucine, methionine, and phenylalanine, were used as the samples for the proof of concept. The possibility of directly detecting these target amino acids from serum samples

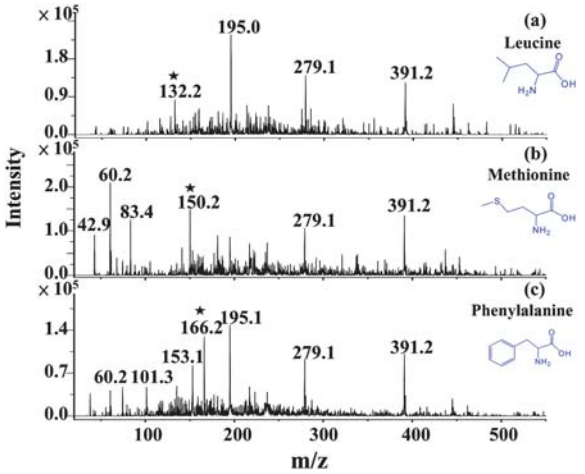

Fig. 5 TDAMS spectra obtained from serum samples (2 μL) spiked with (a) leucine (10^{-6} M), (b) methionine (10^{-5} M), and (c) phenylalanine (10^{-4} M). No sample treatment was made prior to the mass spectral analysis. Amino acid ion peaks were marked with asterisks.

without any sample pretreatment using ambient MS was investigated. It is significant to monitor the presence of these amino acids in the serum samples of newborn babies because these are important indications of metabolism.[33] For example, high concentrations (>1000 μM) of leucine are found in the serum of newborn babies suffering from maple syrup urine disease.[34] Extracting target amino acids from complex serum samples is a conventional step required prior to MS analysis. We believe our approach can eliminate these tedious steps for shortening the analysis time. Fig. 5a–5c show the TDAMS spectra of leucine, methionine, and phenylalanine analyzed directly from diluted serum samples without any sample pretreatment. The pseudo-molecular ions derived from leucine, methionine, and phenylalanine marked with asterisks appear in the mass spectra. Because the composition of serum is quite complicated, there are many background ions derived from the serum matrix revealing in the mass spectra. Nevertheless, protonated amino acid ions can be observed in the mass spectra. The results indicate that TDAMS can be used to detect traces of amino acids directly from complex serum samples without the requirement of any time-consuming pretreatment steps.

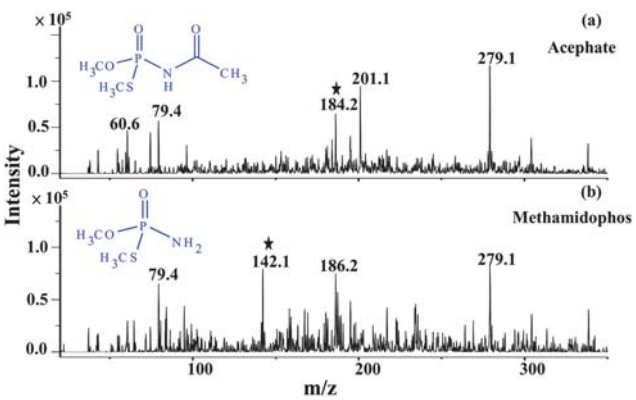

Fig. 6 TDAMS spectra obtained directly from grass immersed in (a) acephate (1 ppm, mw = 183.2) and (b) methamidophos (10 ppm, mw = 141.1) for 60 min. Insecticide ion peaks were marked with asterisks.

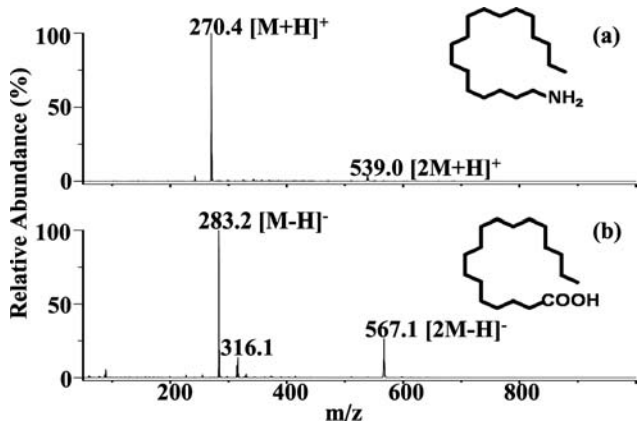

Fig. 7 TDAMS spectra of (a) octadecylamine (1 mM, 2 μL)) and (b) octadecanoic acid (1 mM, 2 μL)).

Polar organophosphate insecticides were also used as samples for examination. We demonstrated that our approach could be readily used to analyze these types of polar compounds including thiabendazole, diazinon, acephate, and methamidophos (results not shown). The detection limit of these insecticides is as low as 10 pg (10 ppb, 1 μL). To demonstrate that these insecticides could be directly analyzed from plants, we immersed grass in a solution containing traces of the insecticides for 60 min followed by placing the grass on the Glass@AuNPs chip for TDAMS analysis. Fig. 6a and 6b present the TDAMS spectra of acephate and methamidophos directly analyzed from the grass, respectively. Their protonated pseudomolecular ions at *m/z* 184.2 and 142.1 marked with asterisks appear in the mass spectra. The results demonstrate that this approach can be used practically to analyze traces of organophosphate insecticides directly from the surface of the grass. The results also demonstrate that our current approach can be used to detect selectively target analytes without any sample treatment.

In addition to small polar analytes organics, analytes with lower polarities were examined by TDAMS. Alkylamines and alkylacids with different lengths of alkyl group (C_{12}–C_{18}) were selected as the samples. These organics can be readily observed in the TDAMS spectra. We only show the mass spectral results of octadecylamine and octadecanoic acid herein (see Fig. 7). The protonated pseudomolecular ions ($[M + H]^+$) and dimer ions ($[2M + H]^+$) of octadecylamine at *m/z* 270.4 and 539.0, respectively, appear in Fig. 7a. Fig. 7b displays the mass spectrum of octadecanoic acid. The deprotonated pseudomolecular ions ($[M - H]^-$) and dimer ions ($[2M - H]^-$) of octadecanoic acid appear at *m/z* 283.2 and 567.1, respectively. The results indicate that TDAMS is also suitable for these lower polarity molecules.

On the basis of the results demonstrated above, TDAMS seems lacking the capability of analyzing organic salts and relatively high polar analytes, which can be readily achieved by existing thermal ionization MS approaches such as ATPDI. Nevertheless, this feature also leads TDAMS to be capable of being used in direct analysis of target analytes with lower polarities from complex samples without sample pretreatment. That is, on the basis of the results shown in Fig. 7, this ambient MS method may be suitable for the analysis of biodiesel samples because the polarity of the expected biodiesel products is usually low. We generated biodiesel samples by treating soybean oil through transesterification reactions. Purifications of the biodiesel product by solvent extraction are generally required prior to MS analysis.[35,36] However, since one of the advantages of TDAMS is its selectivity for the detection of smaller and less polar molecules, the reaction product derived from the transesterification reaction of soybean oil without conducting any extraction steps was examined. Scheme 3 depicts the

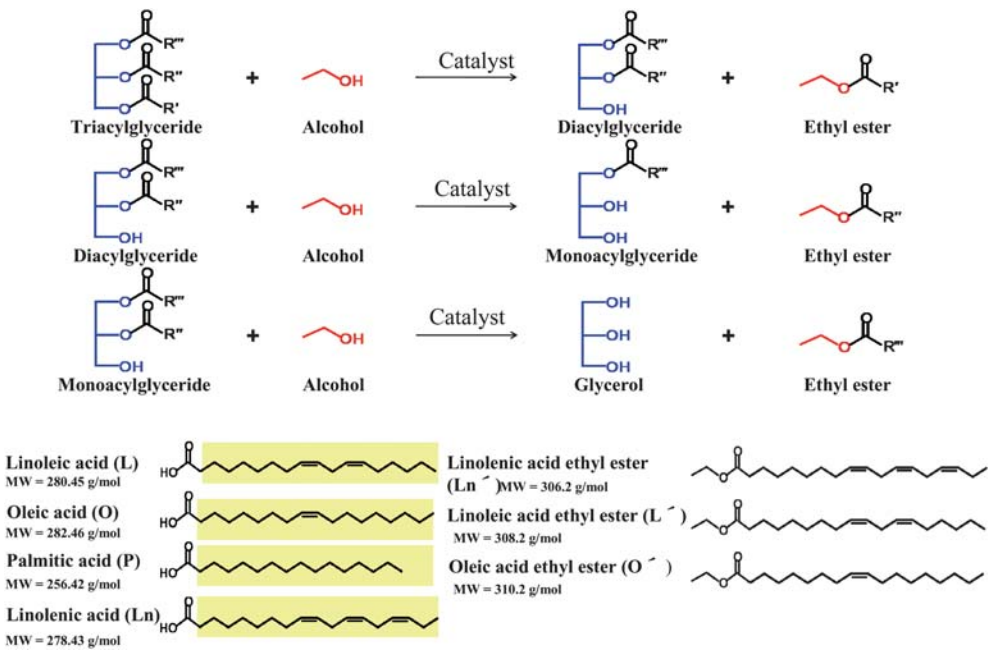

Scheme 3 Transesterification reaction of triacylglyceride. The structures of common fatty acids and fatty acid ethyl esters are also listed. Yellow highlights indicate R′, R″, or R‴.

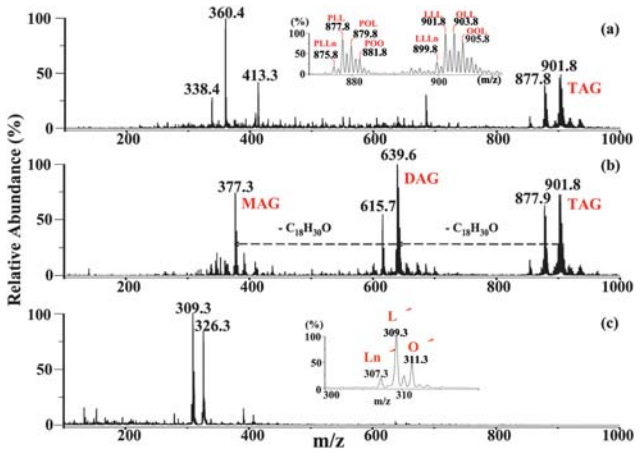

Fig. 8 (a) ESI mass spectrum of soybean oil, (b) ESI mass spectrum of the transesterification product of soybean oil, and (c) TDAMS spectrum of the transesterification product of soybean oil. The product was diluted with 2-propanol 1000-fold without any treatment prior to MS analysis. Target mass was set at *m/z* 500.

representative reactions of the transesterification of triacylglyceride (TAG)[35,37] referred to in this study. TAG, which is one of major compositions in soybean oil, encounters transesterification in the presence of NaOH (catalyst) and ethanol. The carbon chain number in the alkyl (R) group and the number of double bonds in the straight-chain are varied in TAG (see Scheme 1). Ethyl esters are the resultant biodiesel. Fig. 8a presents the ESI mass spectra of soybean oil. Two series of sodiated TAG species appear at *m/z* above 800. The details of the TAG compositions are marked on the mass spectrum as the inset. All the English letters can be referred to those listed in Scheme 3. Fig. 8b displays the ESI mass spectrum of the transesterification product of soybean oil. There is a group of sodiated diacylglyceride (DAG) ions revealing at around *m/z* 615.7 and 639.6, which correspond to the loss of a [Linoleic acid-OH] ($C_{18}H_{30}O$), from the ions derived from sodiated TAG at around *m/z* 877.9 and 901.8, respectively. Furthermore, sodiated monoacylglyceride (MAG) ions appearing at around *m/z* 377.3 were also observed in the same mass spectrum by the loss of one more [Linoleic acid-OH]. However, the expected biodiesels, *i.e.* ethyl esters, were not observed in the lower mass region of the mass spectrum. When TDAMS was used for the analysis of the same sample as used for obtaining Fig. 8b, the biodiesel product, *i.e* fatty acid ethyl ester, revealing at around *m/z* 309.3 dominates the mass spectrum. The details of the ion peaks were depicted as the inset. All the English letters can be referred to Scheme 1. The mass spectrum looks quite clean compared with the mass spectrum shown in Fig. 8b. This is because TDAMS is only capable of selectively detecting smaller molecules. This feature means the biodiesel product can be clearly observed in the TDAMS spectrum without the requirement of conducting any sample extraction steps. The results demonstrate that TDAMS can be directly employed to the analysis of crude biodiesel products.

Conclusions

We have demonstrated a new ambient MS method, which is mainly dedicated towards small organics. The results show that Glass@AuNPs-assisted TDAMS is suitable for the analysis of small organics with low to high polarity including alkylamines, alkylacids, ethyl esters, small organic acids, amino acids, and organophosphate insecticides. Furthermore, without sample pretreatment, the target analytes from complex samples can be readily observed in the mass spectra using this approach. Without performing tedious separation steps, the biodiesel products can be readily observed in the mass spectra using this approach. This approach is suitable to being used for quickly examining whether a reaction successfully proceeds. That is, sample pretreatment and extraction are not required in this approach. The operation of this approach is very straightforward. Generally, adjusting the angle of the laser focusing beam for sample irradiation in several types of ambient MS is critical. However, it is not an issue in this approach. As long as the NIR laser is placed a few mm below the Glass@AuNPs chip, the sample on the upper side of the chip can be readily liberated from the chip through thermal desorption. Although it requires some efforts for fabrication of the Glass@AuNPs chip, the chip can also be repeatedly used by cleaning its surface with suitable solvents after analysis. The sensitivity of TDAMS is as low as 200 fmol for some specific analytes. In terms of sensitivity, speed of analysis, and simplicity of operation, TDAMS is comparable to existing techniques. Thus, the advantages of this ambient MS include speed, ease of operation, selectivity for small and low polarities of analytes, and elimination of sample pretreatment steps. We believe that this approach can be further extended to the rapid screening of various types of small organics such as drugs and organic toxicants, which may be frequently found in complex matrices.

Acknowledgements

We thank the National Science Council of Taiwan for supporting this research financially.

References

1 H.-Y. Lin, C.-T. Chen and Y.-C. Chen, *Anal. Chem.*, 2006, **78**, 6873–6878.
2 C.-L. Kuong, W.-Y. Chen and Y.-C. Chen, *Anal. Bioanal. Chem.*, 2007, **387**, 2091–2099.
3 J. A. McLean, K. A. Stumpo and D. H. Russell, *J. Am. Chem. Soc.*, 2005, **127**, 5304–5305.
4 E. T. Castellana and D. H. Russell, *Nano Lett.*, 2007, **7**, 3023–3025.
5 Y.-F. Huang and H.-T. Chang, *Anal. Chem.*, 2006, **78**, 1485–1493.
6 C.-L. Su and W.-L. Tseng, *Anal. Chem.*, 2007, **79**, 1626–1633.
7 Y.-F. Huang and H.-T. Chang, *Anal. Chem.*, 2007, **79**, 4852–4859.
8 H. Kawasaki, T. Sugitani, T. Watanabe, T. Yonezawa, H. Moriwaki and R. Arakawa, *Anal. Chem.*, 2008, **80**, 7524–7533.
9 J. Sunner, E. Dratz and Y.-C. Chen, *Anal. Chem.*, 1995, **67**, 4335–4342.
10 M. J. Dale, R. Knochenumss and R. Zenobi, *Anal. Chem.*, 1996, **68**, 3321–3329.
11 M. Schurenberg, K. Dreisewerd and F. Hillenkamp, *Anal. Chem.*, 1999, **71**, 221–229.
12 C.-T. Chen and Y.-C. Chen, *Rapid Commun. Mass Spectrom.*, 2004, **18**, 1956–1964.
13 C.-T. Chen and Y.-C. Chen, *Anal. Chem.*, 2005, **77**, 5912–5919.
14 W.-Y. Chen and Y.-C. Chen, *Anal. Bioanal. Chem.*, 2006, **386**, 699–704.
15 N. Malikova, I. Pastoriza-Santos, M. Schierhorn, N. A. Kotov and L. M. Liz-Marzán, *Langmuir*, 2002, **18**, 3694–3697.
16 C. Jiang, S. Markutsya and V. V. Tsukruk, *Langmuir*, 2004, **20**, 882–890.

17 C. Lu, H. Mo1hwald and A. Fery, *J. Phys. Chem. C*, 2007, **111**, 10082–10087.
18 Z. Takats, J. M. Wiseman, B. Gologan and R. G. Cooks, *Science*, 2004, **306**, 471–473.
19 R. B. Cody, J. A. Laramee and H. D. Durst, *Anal. Chem.*, 2005, **77**, 2297–2302.
20 J. Shiea, M.-Z. Huang, H.-J. Shu, C.-Y. Lee, C.-H. Yuan, I. Beech and J. Sunner, *Rapid Commun. Mass Spectrom.*, 2005, **19**, 3701–3704.
21 C. N. McEwen, R. G. McKay and B. S. Larsen, *Anal. Chem.*, 2005, **77**, 7826–7831.
22 J. Wu, C. S. Hughes, P. Picard, S. Letarte, M. Gaudreault, J. F. Levesque, D. A. Nicoll-Griffith and K. P. Bateman, *Anal. Chem.*, 2007, **79**, 4657–4665.
23 H. Chen, S. Yang, A. Wortmann and R. Zenobi, *Angew. Chem., Int. Ed.*, 2007, **46**, 7591–7594.
24 A. U. Jackson, J. F. Garcia-Reyes, J. D. Harper, J. S. Wiley, A. Molina-Diaz, Z. Ouyang and R. G. Cooks, *Analyst*, 2010, **135**, 927–933.
25 R. Haddad, R. R. Catharino, L. A. Marques, M. N. Eberlin and N. Marcos, *Rapid Commun. Mass Spectrom.*, 2008, **22**, 3662–3666.
26 (*a*) H. Chen, Z. Ouyang and R. G. Cooks, *Angew. Chem., Int. Ed.*, 2006, **45**, 3656–3660; (*b*) W. P. Peng, M. P. Goodwin, H. Chen, R. G. Cooks and J. Wilker, *Rapid Commun. Mass Spectrom.*, 2008, **22**, 3540–3548; (*c*) I. Cotte-Rodriguez, H. Hernandez-Soto, H. Chen and R. G. Cooks, *Anal. Chem.*, 2008, **80**, 1512–1519; (*d*) H. Chen, L. S. Eberlin, M. Nefliu, R. Augusti and R. G. Cooks, *Angew. Chem., Int. Ed.*, 2008, **47**, 3422–3425; (*e*) F. Basile, S. Zhang, Y.-S. Shin and B. Drolet, *Analyst*, 2010, **135**, 797–803.
27 Y. s. Coello, A. D. Jones, T. C. Gunaratne and M. Dantus, *Anal. Chem.*, 2010, **82**, 2753–2758.
28 G. Frens, *Nat. Phys. Sci.*, 1973, **241**, 20–22.
29 S. Rodrigues, L. C. A. Mazzone, F. F. P. Santos, M. G. A. Cruz and F. A. N. Fernandes, *Braz. J. Chem. Eng.*, 2009, **26**, 361–366.
30 C.-Y. Hong and Y.-C. Chen, *J. Chromatogr., A*, 2007, **1159**, 250–255.
31 Y.-T. Wu and Y.-C. Chen, *Rapid Commun. Mass Spectrom.*, 2006, **20**, 1995–1999.
32 Y.-T. Wu and Y.-C. Chen, *Anal. Chem.*, 2005, **77**, 2071–2077.
33 S. C. Kalhan and D. M. Bier, *Annu. Rev. Nutr.*, 2008, **28**, 389–410.
34 R. Fingerhut, E. Simon, E. M. Maier, J. B. Hennermann and U. Wendel, *Clin. Chem.*, 2008, **54**, 1739–1741.
35 R. R. Catharino, H. M. S. Milagre, S. A. Saraiva, C. M. Garcia, U. Schuchardt, M. N. Eberlin, R. Augusti, R. C. L. Pereira, M. J. R. Guimarães, G. F. deSa', J. M. R. Caixeiro and V. Souza, *Energy Fuels*, 2007, **21**, 3698–3701.
36 I. Eide and K. Zahlsen, *Energy Fuels*, 2007, **21**, 3702–3708.
37 B. Freedman, R. O. Butterfield and E. H. Pryde, *J. Am. Oil Chem. Soc.*, 1986, **63**, 1375–1380.